Mecatronics-REM 2012
November 21-23, 2012, Paris, France

Evaluation of a Betaless Instantaneous Cornering Stiffness Estimation Scheme for Electric Vehicles

A. Viehweider, K. Nam, H. Fujimoto, Y. Hori
Hori Fujimoto laboratory, Department of Advanced Energy
The University of Tokyo
Kashiwa, Japan
viehweider@ieee.org

***Abstract*—This contribution evaluates a new Beta-less Instantaneous Cornering Stiffness (ICS) estimation scheme. It relies on the availability of the lateral tire forces measurement which in near future can be realized with economic (low cost) sensors. The estimation is only available if the change in the tire slip angle is profound enough as it is not the case during constant cornering. However, as it is shown with simulation and experimental results the ICS can be estimated in important vehicle dynamic situation and the information used for lateral tire force saturation detection and control. Additionally, it could be used to shorten the convergence time of "linear" cornering stiffness estimation schemes. Since it requires some derivatives of measured signals, a special signal processing techniques must be applied to overcome inaccuracy due to sensor noise.**

Keywords—Lateral vehicle dynamics; Electric vehicle; Instantaneous Cornering Stiffness; Control Allocation

I. INTRODUCTION

Ground vehicle cornering stiffness estimation is a well established field in vehicle control engineering. The knowledge of the front and rear cornering stiffness estimation allow the parametrization of the so called bicycle model (Fig. 1) of the vehicle and the use of this model for control purposes. However, one main difficulty in this regard is the availability of the body slip angle β or the vehicle lateral velocity v_y, which can not be measured at reasonable cost yet. [1] introduces a "beta-less" method and a transfer-function method. By defining intermediate parameters X_1, X_2 and by use of the lateral acceleration and yaw rate measurements together with a Recursive Least Square (RLS) estimator valid identification of the cornering stiffness values is achieved and the validity shown by simulation. This idea has been refined by [2] as far as the use of lateral tire force sensors - which in near future will be available at reasonable costs - is concerned. Often the vehicle is assumed to be in the linear operating range of lateral vehicle dynamics. That means that there is a linear relationship between the tire slip angle of a wheel (Fig. 1 right) and its associated lateral tire force. However, when approaching lateral tire force saturation this assumption is violated and estimation schemes that rely on this assumption give only reduced cornering stiffness values as estimates but are not able to detect imminent lateral tire force saturation and do not reflect this situation well. This information could be vital for an advanced vehicle control system.

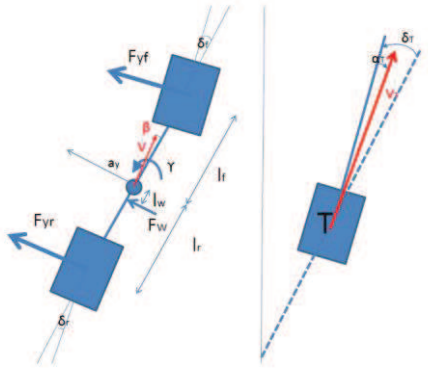

Figure 1. Bicycle model (left) with combined front lateral and rear lateral tire forces and definition of tire slip angle (right). ($\mathbf{a_y}$: lateral acceleration, $\boldsymbol{\gamma}$: yaw rate, $\boldsymbol{\beta}$: body slip angle, $\boldsymbol{\delta_f}$: front steering angle, $\boldsymbol{\delta_r}$: rear steering angle, $\mathbf{F_{y,f}}$: combined front lateral tire force, $\mathbf{F_{y,r}}$: combined rear lateral tire force, $\mathbf{F_w}$: wind disturbance force, $\mathbf{l_f}$: distance of front axle from COG, $\mathbf{l_r}$: distance of rear axle from COG , $\mathbf{l_w}$: distance of aerocenter from COG.

The instantaneous cornering stiffness is defined as the slope of the tire slip angle - lateral tire force relationship at the current tire slip angle. For small tire slip angles it is equivalent to the "linear" cornering stiffness value. For higher tire slip angles it becomes smaller and becomes 0 when lateral tire force saturation is reached and even negative beyond. [3] describes an Instantaneous Cornering Stiffness (ICS) estimation scheme based on a very stringent mass assumption and a special positioning of the lateral acceleration sensor.

In this contribution an advanced beta-less ICS scheme based on the Lateral Tire Force (LTF) measurement is evaluated. The estimation is only available, if the change in the tire slip angle is pronounced enough to guarantee the excitation criteria. However, as shown with simulation and experimental results, the ICS can be estimated in very important situations to avoid lateral tire force saturation. Section 2 discusses the relevant modeling issues and section 3 introduces the ICS schemes. Simulation results for the use of this scheme in a comprehensive control scheme and experimental results for early detection of lateral tire force saturation during vehicle constant cornering with lateral acceleration $a_y > 0.7g$ are given in section 4. Section 5 summarizes and tries to give some

This research has been made possible partly by a JSPS (Japan Society for the Promotion of Science) fellowship and a kakenhi grant with number 24-00760. It was partly supported by the Industrial Technology Research Grant Program from the New Energy and Industrial Technology Development Organization (NEDO) of Japan (number 05A48701d), and by the Ministry of Education, Culture, Sports, Science and Technology grant (number 22246057).

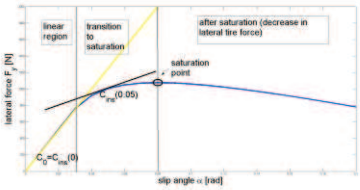

Figure 2. Lateral tire force in dependence of the tire slip angle - „ (defined in the negative sense)

short conclusions and outlooks for future research. In an appendix the used real time derivative estimation method and the particular allocation scheme is further detailed.

II. MODELLING ISSUES

In Fig.1 the relationship between the lateral tire slip angle and the lateral tire force is given. As one can see there is a region where this relationship is linear; the other regions are characterized by a highly non linear behavior of the lateral tire force. The lateral tire force reaches a maximum and for tire slip angles greater than the saturation tire slip angle the lateral tire force may even decrease. Only in the linear region the cornering stiffness values equals to the lateral tire force divided by the negative tire slip angle ($C_{0,\{f,r\}} = -\frac{F_{y,\{f,r\}}}{\alpha_{\{f,r\}}}$). In the other two regions this is not the case, where the ICS represent the slope of this curve at a certain tire slip angle and can be positive, zero and may also be negative. The so called bicycle model is based on the principle that the two front wheels and the two rear wheels are combined into one front and rear wheel (Fig. 1), therefore the combined lateral tire forces are given by:

$$\begin{aligned} F_{y,f} &= F_{y,fl} + F_{y,fr} \\ F_{y,r} &= F_{y,rl} + F_{y,rr} \end{aligned} \tag{1}$$

where $F_{y,fl}, F_{y,fr}, F_{y,rl}, F_{y,rr}$ are the front left, front right, rear left and rear right wheel lateral tire forces.

The dependence of the cornering stiffness on the lateral tire force is in a wide range linear (Fig. 2). Due to load transfer during cornering at constant velocity v_x the cornering stiffness is decreased at one wheel of the axle and at the same time increased at the other wheel of the axle [4]. Therefore it is reasonable to consider the cornering stiffness of the front wheels and the rear wheels together and to combine the front left and right tire force and the rear left and right tire force as done in (1). The tire slip angles of the four wheels are given (derived from kinematic relationships as in [5]):

$$\begin{aligned} \alpha_{f,l} &= -\left(\delta_f - \arctan\frac{v_y+\gamma l_f}{v_x-\frac{d}{2}\gamma}\right), \\ \alpha_{f,r} &= -\left(\delta_f - \frac{\arctan(v_y+\gamma l_f)}{v_x+\frac{d}{2}\gamma}\right), \\ \alpha_{r,l} &= -\left(\delta_r - \frac{\arctan(v_y-\gamma l_r)}{v_x-\frac{d}{2}\gamma}\right), \\ \alpha_{r,r} &= -\left(\delta_r - \frac{\arctan(v_y-\gamma l_r)}{v_x+\frac{d}{2}\gamma}\right), \end{aligned} \tag{2}$$

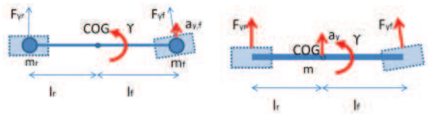

Figure 3. Left: Sensor concept and particular mass assumption for ICS estimation without body slip angle measurement and without lateral tire force measurement (L E) according to III b. Right: Used sensors for estimation scheme according to section III c.

where δ_f, δ_r are the steering angles of the front and rear (In this contribution a vehicle with Active Front and Active Rear Steering (AFS,ARS) is considered.) wheels, v_x, v_y the longitudinal and lateral velocity of the vehicle, γ the yaw rate, l_f, l_r the distance of the front and rear axes from the center of gravity and d the length of the tread.

If the vehicle longitudinal velocity v_x is not too low, one can consider the tire slip angle of the two front wheels and the two rear wheels as equal and approximate the arctan function as following [4]:

$$\begin{aligned} \alpha_f &\approx \alpha_{f,l} \approx \alpha_{f,r} \approx -\left(\delta_f - \beta - \frac{l_f\gamma}{v_x}\right), \\ \alpha_r &\approx \alpha_{r,l} \approx \alpha_{r,r} \approx -\left(\delta_r - \beta + \frac{l_r\gamma}{v_x}\right), \end{aligned} \tag{3}$$

where $\beta \approx \frac{v_y}{v_x}$. The instantaneous front and rear cornering stiffness as opposed to the absolute cornering stiffness is defined as following:

$$C_{ins,\{f,r\}}(\alpha) = -\frac{dF_{y,\{f,r\}}(\alpha_{\{f,r\}})}{d\alpha_{\{f,r\}}}. \tag{4}$$

For tire slip angle $\alpha_{\{f,r\}} = 0$ (and small tire slip angles) instantaneous and absolute cornering stiffness are equal:

$$C_{0,\{f,r\}} \approx C_{ins,\{f,r\}}(0). \tag{5}$$

III. A LTF BASED ICS ESTIMATION SCHEME

The knowledge of the ICS could be used in a vehicle dynamics system to prevent lateral tire force saturation. Before introducing a new method in subsection C, two methods from the literature are shortly explained in subsection A and B:

A. Beta based estimation (recursive least squares based)

If the body slip angle β is known, very small or estimated by some sophisticated interlaced observer-estimation scheme as in [6], the tire slip angles $\alpha_{\{f,r\}}$ can be computed with the measurement of the yaw rate γ and the front and rear steering angles δ_f, δ_r according to (3).

In order to get the ICS a recursive least square estimation scheme can be applied in order to get the instantaneous cornering stiffness $C_{ins,\{f,r\}}$ as done in [6] with:

L f X

L wÆ◊Ý f L >gl ÆÝ ‘ÆÝ ? (6)

L Þ ◊Ý F s ?

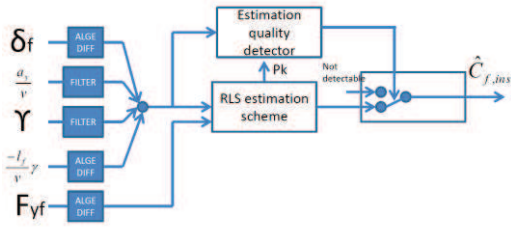

Figure 4. Structure of the front Instantaneous Cornering Stiffness (ICS) estimation

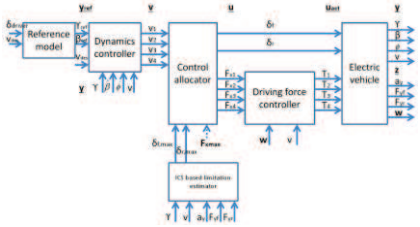

Figure 5. Control scheme for an EV with active front and rear steering and 4 In-Wheel-Motors based on reference model, dynamic controller, control allocator, subordinated driving force controller and limit value generation for control allocator.

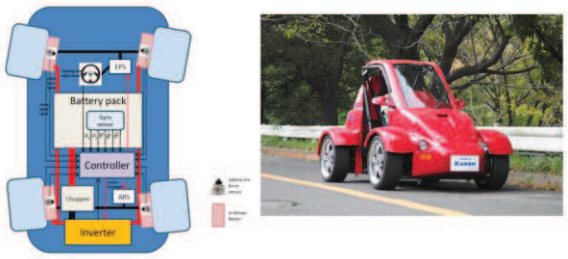

Figure 6. General overview of the test vehicle (left) and picture of test vehicle (right) used for experimental evaluation

Figure 7: Lateral tire force sensor (NSK Ltd.)

B. Previous approach (special mass distribution assumption)

Estimation of the body slip angle is particularly difficult since it requires either an unreasonably expensive sensor or an accurate non linear model of the vehicle or some sophisticated estimation scheme as in [6] or [7]. It would be advantageous to estimate the ICS without the explicit knowledge of the body slip angle. In [3] an estimation scheme for a particular mass distribution assumption and the positioning of a lateral acceleration sensor at the front tread is given. The ICS (From now on only the front ICS is considered, but the derivation is quite similar for the rear ICS) can be approximately estimated by the use of the time derivatives of tire slip angle and tire lateral force in the following way:

$$C_{f,ins}(\alpha) = -\frac{dF_{y,f}(\alpha_f)}{d\alpha_f} = -\frac{\frac{dF_{y,f}}{dt}}{\frac{d\alpha_f}{dt}}. \tag{7}$$

This estimation is valid if

$$\frac{d\alpha_f}{dt} \neq 0. \tag{8}$$

The use of the time derivative of the tire slip angle is advantageous in the sense that no explicit estimation of the body slip angle is necessary, since:

$$\dot{\alpha}_f = -\left(\dot{\delta}_f - \dot{\beta} - \frac{l_f}{v_x}\dot{\gamma}\right), \tag{9}$$

with

$$\beta \approx \frac{a_y}{v_x} - \gamma, \tag{10}$$

which is derived from kinematic relationship, leads to:

$$\dot{\alpha}_f = -\left(\dot{\delta}_f - \frac{a_y}{v_x} + \gamma - \frac{l_f}{v_x}\dot{\gamma}\right). \tag{11}$$

Since practically usable and economic viable tire lateral force sensors will come out in near future, first approaches of cornering stiffness were based on using lateral acceleration at the front axle $a_{y,f}$ together with the already mentioned assumption of a particular mass distribution of the vehicle [3].

If the mass of the vehicle is concentrated at the front and rear axle then the following equation - under the condition that (8) holds true - is a valid estimation value for the ICS [3]:

$$C_{f,ins} \approx \frac{m l_r}{l_f + l_r} \frac{\dot{a}_{y,f}}{\dot{\delta}_f - \frac{\dot{a}_{y,f}}{v_x} + \gamma}, \tag{12}$$

where $a_{y,f} = a_y + \frac{l_f \dot{\gamma}}{v_x}$ is the acceleration of the vehicle measured at the position of the front axle (compare Fig. 3).

C. New approach (lateral tire force sensor based)

Since the aforementioned mass assumption may be violated, in this contribution an approach based on the use of lateral tire force sensors (see Fig. 7 for the concrete appearance of a sensor of this kind) is suggested which is generally valid and not only for a particular mass distribution assumption. The use of lateral tire force sensors as depicted in Fig. 4 allows to get rid of the special mass assumption and the determination of the ICS via the following equation:

$$C_{f,ins} \approx \frac{\dot{F}_{y,f}}{\dot{\delta}_f - \frac{a_y}{v_x} - \gamma - \frac{l_f}{v_x}\dot{\gamma}} = \frac{\dot{y}}{\dot{x}}, \tag{13}$$

if (8) holds true. This is a pure analytical result and does not take into account the challenges the practical implementation introduces. At first (13) relies on real time derivatives of the steering angle δ_f, the yaw rate γ and the lateral tire force sensor signal $F_{y,f}$. These signals may be noisy (especially the lateral tire force signal). As a consequence special signal processing is needed. As a particular suited filtering technology the Algebraic Real Time Derivative Estimation technique has been used to compute the time derivative of the noisy signals in general. More details are given in the appendix.

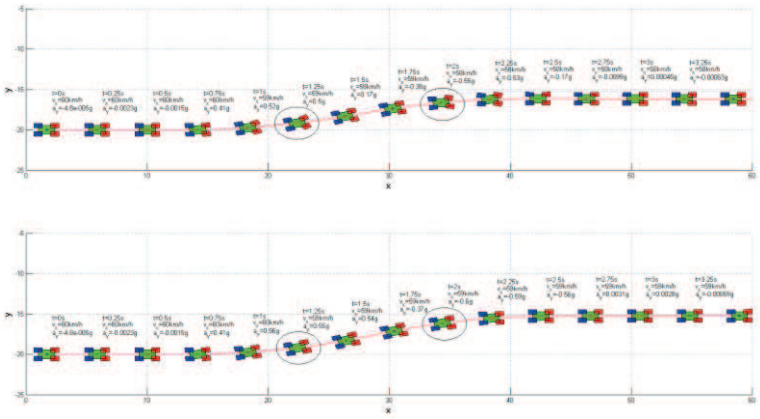

Figure 8. Comparison of trajectories resulting from control without ICS information (upper) with ICS information (lower) for the lane change maneuvers at a speed of $\mathbf{60km/h}$ and road condition $\boldsymbol{\mu = 0.65}$.

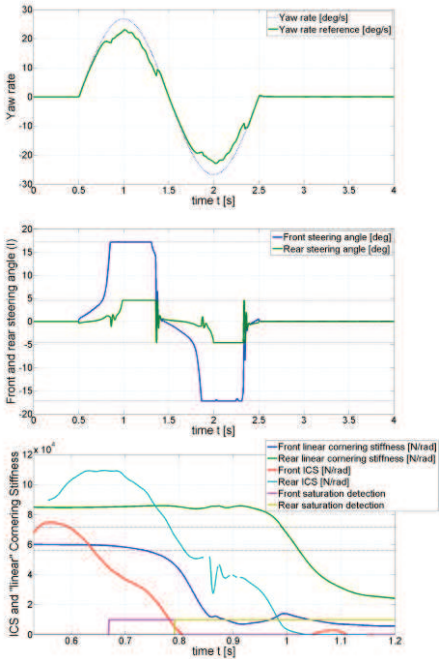

Figure 9. Relevant signals (top: yaw rate, middle: steering angles, bottom: linear cornering stiffness values and ICS values) without use of ICS information for the lane change manoeuvre at a speed of $\mathbf{60\ km/h}$ and road condition $\boldsymbol{\mu = 0.65}$.

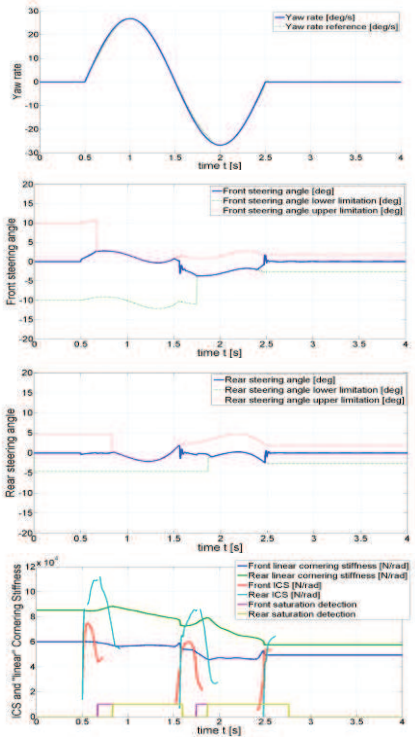

Figure 10. Relevant signals (top: yaw rate, middle: steering angles, bottom: linear cornering stiffness values and ICS values) with use of ICS information for the lane change manoeuvre at a speed of 60 km/h and road condition μ =0.65.

Additionally in order to avoid the explicit division of two quantities heavily affected by noise the estimation is embedded in a standard RLS estimation scheme(as for example described in [8]) with $y = \dot{F}_{y,f}$,$x = -\dot{\alpha}_f$ and $\theta = C_{f,ins}$:

$$\begin{aligned} \Pi_k &= \frac{P_{k-1}x_k}{\lambda + P_{k-1}x_k^2} \\ \Theta_k &= \Theta_{k-1} + \Pi_k(y_k - \Theta_{k-1}x_k) \\ P_k &= \frac{1}{\lambda}(P_{k-1} - \Pi_k x_k P_{k-1}) \end{aligned} \qquad (14)$$

with $\theta_0 = 0$ and λ (forgetting factor), P_0 adequately chosen. The RLS scheme avoids the explicit division, although estimation quality during low values of $|\dot{\alpha}_f|$ may also be poor. Therefore it is advisable to detect low values of $|\dot{\alpha}_f|$ and not to trust the estimation in this case.

Actually the decision (compare Fig. 4) when the ICS estimation is valid has been based in this contribution on a criteria that combines the information when amount of the denominator in (13) is large enough and at the same time the

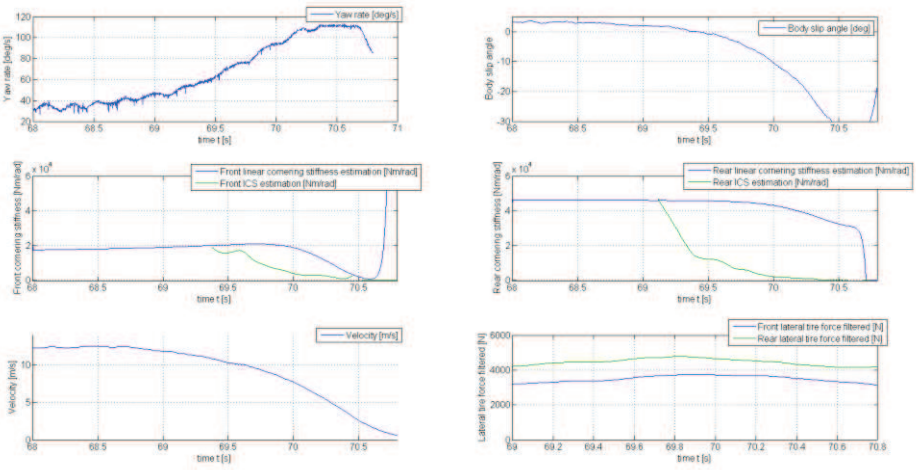

Figure 11. Vehicle signals and estimated cornering stiffness values - constant cornering around 40 km/h at a dry road before loss of stability.

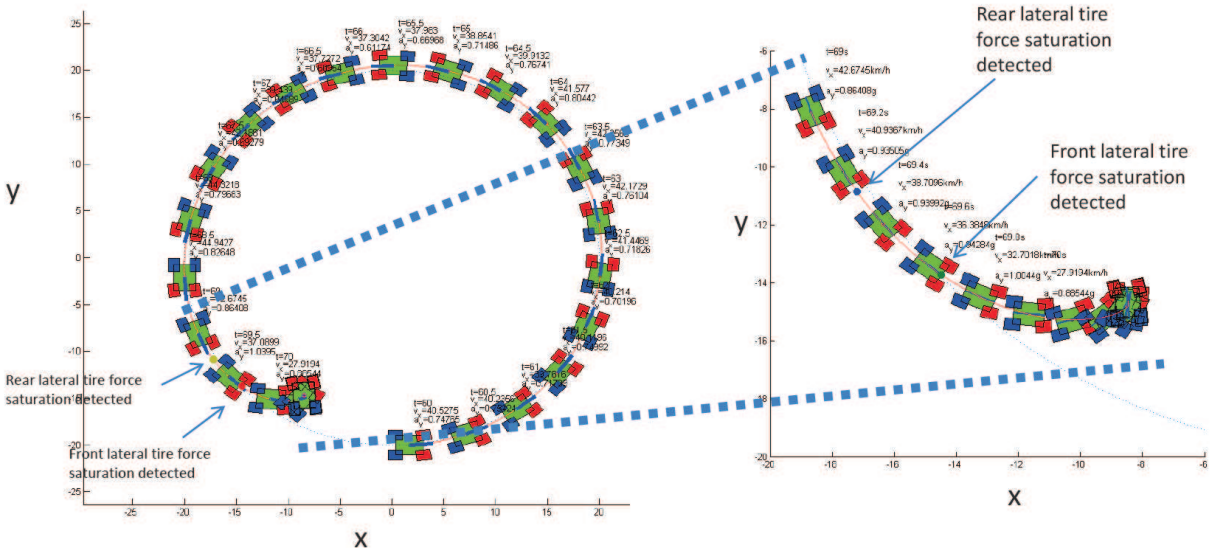

Figure12. Trajectories from experimental validation - constant cornering around 40 km/h before loss of stability.

estimated covariance P_k from the RLS estimation is small enough in order to trust the estimated parameter (the ICS value), i.e.:

$$\hat{C}_{f,ins} = \begin{cases} \theta_k & (|\dot{\alpha}_f| > s_\alpha) \Lambda (P_k < P_{lim}) \\ \text{not defined} & otherwise \end{cases}, \quad (15)$$

with s_α and P_{lim} appropriately chosen.

IV. Simulation and Experimental Results

For the simulation and the experiment the parameters of the considered test vehicle are as follows: $m = 880kg$, $J_z = 562kgm^2$, $l_f = 0.999m$, $l_r = 0.701m$ and wheel base $l_r = 1.3m$. The simulation has been carried with the commercial simulation package CarSim and the real life experiment on a special test track due to safety concerns with a test vehicle available at our laboratory.

A. Simulative evaluation of the ICS estimation scheme in a comprehensive control scheme for a lane change manoeuvre

In a simulation based evaluation of the ICS estimation scheme the knowledge of the front and rear ICS values have been used to prevent the vehicle reaching lateral tire force saturation. The estimation scheme is embedded in an Electric Vehicle control concept that consists of reference model, dynamic controller, control allocator, subordinated driving force controller and the ICS based steering angle limitation estimator as shown in Fig. 5. The electric vehicle is equipped with Active Front Steering (AFS) and Active Rear Steering (ARS) and 4 In-Wheel-Motors (IWMs) (6 degrees of freedom)

(Fig. 5). The control allocation concept is shortly described in appendix B. For more information on allocation based vehicle dynamics control system confer [8], [9] and [10].

The controller tries to track the desired yaw rate γ_{ref} and body slip angle β_{ref} from the reference model that are derived from the driver steering angle and velocity and keeping the velocity at 60km/h and suppress excessive roll motion by acting on all 6 actuators. However, since the road is slightly slippery ($\mu = 0.65$), during the lane track manoeuvre the vehicle may run into lateral tire force saturation. Two cases are compared: In the first scheme the controller is given no explicit information about the ICS, the steering angle limits for the control allocator are the physical ones, in the second scheme the ICS is estimated and a big decrease interpreted as *imminent lateral tire force saturation* and from this maximal allowable slip angle bounds for the steering angles derived. This means that the control allocator is aware of these bounds and should the yaw moment generated by steering not suffice due to the calculated limits, the allocator can apply additional yaw moment generated by particular 4 wheel driving force distribution. In Fig. 8, Fig. 9 and Fig. 10 results for the two schemes are shown. With the first scheme (Fig. 9 top) the yaw rate reference tracking is poor and the steering actuators (Fig. 9 middle) saturate and remain within saturation between 0.8s and 1.35s and between 1.8s and 2.3s. With the second scheme the yaw rate tracking is quite good (Fig. 10 top). As soon as the estimated ICS values drop to a certain percentage of the maximum (Fig. 10 bottom) the steering angle limit values for the allocators are reduced (Fig. 10 middle). In Fig. 10 bottom the ICS values are given. As described in section 3 the ICS estimate is only available at certain times (15). In this sub figure also the cornering stiffness based on a linear model (as in [1]) is given. As expected it does not describe the dynamic situation of the vehicle well. As the lateral tire force saturates, the "linear" cornering stiffness estimation leads to reduced values of the estimated cornering stiffness but with a long convergence time. Therefore a changing road condition or imminent tire force saturation cannot really be discriminated. *Furthermore, the detection of imminent lateral tire force saturation with the linear cornering stiffness takes at least* 0.2s *longer which is from the perspective of lateral vehicle dynamics unacceptable.*

The ICS estimation is very fast, but cannot be applied during stationary operation (constant tire slip angle). It is highly probable that by combining the "linear" estimator for cornering stiffness with the ICS estimation scheme, the cornering stiffness estimation can be improved even in the linear domain leading to a faster convergence time and at the same time getting good estimates even if there is no change in tire slip angle. In Fig. 8 the trajectories for the two cases are given. It can be seen that without the use of the ICS information the trajectory differs significantly and the actuators reach extreme values at certain time instants (encircled).

B. *Experimental evaluation of the ICS estimation scheme for early lateral tire force detection during constant cornering*

The experimental evaluation consists of an early detection of the lateral tire force saturation of an electric test vehicle (as shown in Fig. 12) without dynamic control based on the ICS estimation with LTFS during constant cornering ($r = 20\text{m}$) at a velocity $v_x \approx 40\text{km/h}$ and a lateral acceleration $a_y \approx 0.7\text{g}$. The road condition can be considered as ideal (a high μ value) and the front steering angle kept constant at $\delta_f = 7.45\text{deg}$. The vehicle uses only front steering and rear wheel traction (no rear wheel steering and no front wheel traction). In Fig. 12 the trajectory together with the steering angle of the wheels are shown. The rear wheels reach earlier the lateral tire force saturation ($t \approx 69.3\text{s}$) due to rear wheel traction (friction circle!) and slight deceleration since at time $t = 68.5\text{s} \ldots 69.5\text{s}$ the vehicle slightly decelerates (load transfer!).

In Fig. 11 the estimated ICS together with the results from an estimator based on a the linear assumption are shown. It goes without saying that during constant cornering the ICS estimation is not available since the tire slip angles are nearly constant. When the ICS estimation becomes possible the estimation values fit quite well with the estimation from the "linear" scheme. The rear ICS decreases very fast, the front ICS takes longer. If a decrease to 60% in the ICS is considered as an indicator for imminent lateral tire force saturation, in Fig. 12 the location of the COG of the vehicle at times at which the rear and front lateral tire force saturation is detected, is indicated. Especially the rear one can be detected very early and appropriate countermeasures could be taken in order to prevent the vehicle to become unstable. Again as in the simulation example (section 4.1) it is not possible to detect this kind of imminent instability with an estimation scheme based on the linear assumption. *If a decrease of* 10% *of the linear cornering stiffness value is interpreted as imminent lateral tire force saturation the detection time is in this example at least* 0.3s *higher without the use of ICS.*

In the derivation up to now the vehicle velocity v_x has been assumed to be constant or only slow time varying. This assumption may be violated after time instants $t > 69.7s$. However the saturation has already been detected before. The vehicle signals (yaw rate γ, longitudinal velocity v_x and lateral tire force sensor signals F_{yf}, F_{yr} have been real time filtered. The test vehicle has been equipped with a body slip angle measurement device (optical); therefore, the body slip angle was available and shown in Fig. 11, but not used for the tire force saturation detection scheme.

V. CONCLUSIONS

This contribution introduced and evaluated an ICS estimation scheme that does not rely on explicit or implicit knowledge of the body slip angle, but uses information from the lateral tire force sensor. The ICS estimation is valid if the change in the tire slip angle is profound enough. Since it relies on the determination of time derivatives of noisy sensor signals and a quotient of two noisy quantities appropriate signal processing techniques are necessary.

The information of the ICS can be used for detection and control. The detection of imminent lateral tire force saturation is more reliable and in the discussed maneuvers at least 0.2s faster than the conventional scheme. Since EV may offer a high degree of actuation, ICS information can play a vital role in the allocation process.

Future topics will be the explicit consideration of tire longitudinal and lateral saturation coupling and its impact on the comprehensive control scheme. This problem has not been addressed in this contribution and is worthwhile to be discussed.

ACKNOWLEDGMENT

This research has been made possible partly by a JSPS (Japan Society for the Promotion of Science) fellowship and a kakenhi grant with number 24-00760. It was partly supported by the Industrial Technology Research Grant Program from the New Energy and Industrial Technology Development Organization (NEDO) of Japan (number 05A48701d), and by the Ministry of Education, Culture, Sports, Science and Technology grant (number 22246057).

REFERENCES

[1] C. Sierra, E. Tseng, A. Jain, and H. Peng, "Cornering stiffness estimation based on vehicle lateral dynamics," Vehicle System Dynamics: International Journal of Vehicle Mechanics and Mobility, vol. 44, pp. 24-38, 2006.

[2] B. M. Nyguyen, K. Nam, H. Fujimoto, and Y. Hori, "Proposal of Cornering Stiffness Estimation without Vehicle Side Slip Angle using Lateral Force Sensor," IIC, pp. 1-6, 2011.

[3] W. Sienel, "Estimation of the tire cornering stiffness and its application to Active Car Steering," Proc. of the 36th Conference on Decision and Control, San Diego, California, pp. 4744-4748, 1997.

[4] H. B. Pacejka, Tyre and Vehicle Dynamics, Elsevier, Butterworth-Heinemann, 2006.

[5] S. Antonov, Model-based Vehicle Dynamics Control, Phd thesis, Automation Control Institute, University of Technology Vienna, Austria, 2008.

[6] L. Haffner, M. Kozek, J. Shi, and H. P. Joergl, "Estimation of the maximum friction coefficient for a passenger vehicle using the instantaneous cornering stiffness," Proc. of the American Control Conference, Seattle, Washington, pp. 4591-4596, 2008.

[7] C. Geng and Y. Hori, "Nonlinear Body Slip Angle Observer for Electric Vehicle Stability Control,", Proc. of the EVS 23, 2008.

[8] L. Xiong and Z. Yu, "Control Allocation of Vehicle Dynamics Controlfor a 4 In-Wheel-Motored EV," Proc. of the International Conference on Power Electronics and Intelligent Transportation System, pp. 307-311, 2009.

[9] J. Krueger, A. Pruckner and C. Knobel, "Control Allocation for Road Vehicles - a system-independent approach for integrated vehicle dynamics control," Proc. of 19. Aachener Kolloqium Fahrzeug- und Motorentechnik 2010, pp. 1-13, 2010.

[10] A. Viehweider and Y. Hori, "Electric Vehicle Lateral Dynamics Control based on Instantaneous Cornering Stiffness Estimation and an Efficient Allocation Scheme," Mathmod Conference, Vienna, Austria, 2012.

[11] M. Fliess, M. Mboup, H. Sira-Ramirez, Analyse et representation de signaux transitories: application a la compresion, au debruitage, et a la detection de rupture, GRETSI 2005, Belgium, 2005.

[12] J. Zehetner and M. Horn, "Echtzeitableitungsschaetzung am Beispiel automotiver Anwendungen," Proc. of the Retzhof Symposium 2007, Rezthof Leibniz, Austria, 2007.

[13] E. Katsuyama, "Decoupled 3D Moment Control by In-Wheel Motor", EVTech2011, JSAE Spring Meeting, Yokohama, Japan, 2011.

[14] O. Haerkeg°ard, Backstepping and Control Allocation with Applications to Flight Control, Department of Electrical Engineering, Linkoeping University, PhD Thesis, 2003.

APPENDIX

A. Algebraic Real Time Derivative Estimation

As especially helpful in the real time determination of the time derivative algebraic based methods as introduced in [11] and [12] have been turned out. The basics are summarized shortly in this section. For more information confer [12]: Based on the theoretical foundation of Fliess [11] main idea is to approximate the signal within a certain interval with a Taylor series and to make use of the Laplace transformation to determine the *k*th coefficient of the Taylor series which locally (t = 0) corresponds to the value of the kth derivative. Exemplary the Taylor series for a signal is [12]:

$$y(t) = \sum_{i=0}^{n} \frac{c_i}{i!} t^i, \tag{16}$$

and its second order approximation:

$$y(t) = c_0 + c_1 t + c_2 t^2. \tag{17}$$

The Laplace transformation leads to [12]:

$$Y_2(s) = \frac{c_0}{s} + \frac{c_1}{s^2} + \frac{c_2}{s^3}. \tag{18}$$

After some elementary operations (differentiation and multiplication with some order of s), c_1 can be determined by following equation:

$$\frac{1}{s^5} c_1 = -\frac{3}{s^3} Y_2(s) - \frac{5}{s^2} \frac{d}{ds} Y_2(s) - \frac{1}{s} \frac{d^2}{ds^2} Y_2(s). \tag{19}$$

The back transformation in the time domain leads to following expression [12]:

$$c_1 = \int_0^t \Pi(t,\tau) y_2(\tau) d\tau = \tag{20}$$

$$= \int_0^t \frac{1}{t^4} (-36(t-\tau)^2 + 120(t-\tau) - 24\tau^2) y_2(\tau) d\tau.$$

The parameter t must be a compromise between noise attenuation and accuracy of the taylor approximation and the computational effort, since for real implementation the integral has to be approximated in the Riemann sense as a finite sum. Since for real time applications, future values are not known, the Taylor approximation from former values has to be used. This leads to following approximation of the first derivative at discrete time instants l [12]:

$$y_l^{(1)} = \frac{T_S}{2} \sum_{i=1}^{F} \Pi_{i-1} y_{l-i+1} + \Pi_i y_{l-i},$$
$$\Pi_i = \frac{1}{F^4 T_S^2} [36(F-i)^2 - 120(F-i)i + 24i^2]. \tag{21}$$

where T = FTs is the window size for Taylor approximation, which must be chosen carefully. (Ts: sampling time, F: discrete window width).

In Fig. 14 comparison results are shown between (higher order filtering + difference) and Algebraic Real Time derivative Estimation (ARTE) computation. In both cases the window size has been chosen as T = 1s.

The cut off frequency of the higher order filter has been chosen in order to minimize the MSE error and is different in the two cases.

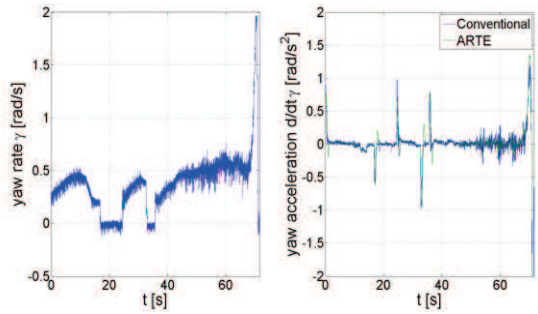

Figure 13. Real time yaw rate time derivative computation with ARTE

It is a compromise in between suppressing ripple of the signal and not to introduce to much phase lag. It is shown that in both the cases the ARTE approach with the same window size outperforms the conventional derivative computation with filtering. In Fig. 13 the application to the yaw rate signal of the experimental evaluation is shown.

B. Control Allocation Based Vehicle Controller

The control scheme as shown in Fig. 4 has as its core a control allocator. The allocation scheme is based on the allocation of the front and rear lateral forces and the four driving (longitudinal) forces of each wheel (subordinate controller translate the force demand into steering angles and motor torques):

$$\mathbf{v} = \mathbf{B}\mathbf{u},$$

$$\begin{bmatrix} v_1 \\ v_2 \\ v_3 \\ v_4 \end{bmatrix} = \begin{bmatrix} a_y \\ \gamma_{ref} \\ F_x \\ M_x \end{bmatrix} = \begin{bmatrix} \frac{1}{m} & \frac{l_f}{J_z} & 0 & 0 \\ \frac{1}{m} & -\frac{l_r}{J_z} & 0 & 0 \\ 0 & -\frac{d}{2J_z} & 1 & -\frac{d\tan(\theta_f)}{2} \\ 0 & \frac{d}{2J_z} & 1 & \frac{d\tan(\theta_f)}{2} \\ 0 & -\frac{d}{2J_z} & 1 & \frac{d\tan(\theta_r)}{2} \\ 0 & \frac{d}{2J_z} & 1 & -\frac{d\tan(\theta_r)}{2} \end{bmatrix}^T \begin{bmatrix} F_{y,f} \\ F_{y,r} \\ F_{x,1} \\ F_{x,2} \\ F_{x,3} \\ F_{x,4} \end{bmatrix}, \quad (22)$$

where $\mathbf{v}$ are the control signals from the higher level controller and θ_f, θ_r are the anti-dive and anti-lift angles of the IWMs. In the considered case the controller gives demand for lateral acceleration, yaw acceleration, longitudinal force and additional roll moment due to the so called anti-dive and anti lift forces due to the particular suspension of the IWM driven vehicle (for more information confer [13]).

Lateral and longitudinal tire forces can saturate, therefore, these limits should be considered in the allocation scheme:

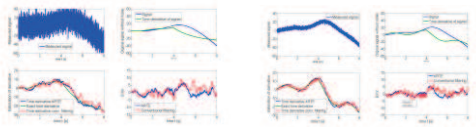

Figure 14. Comparison of ARTE approach with higher order conventional filter and difference quotient for estimation of time derivative of a highly noisy signal with optimized cut off frequency of higher order filter for minimal MSE error.

$$\begin{bmatrix} F_{y,fmin}(t) \\ F_{y,rmin}(t) \\ F_{x,1min}(t) \\ F_{x,2min}(t) \\ F_{x,3min}(t) \\ F_{x,4min}(t) \end{bmatrix} < \begin{bmatrix} F_{y,f} \\ F_{y,r} \\ F_{x,1} \\ F_{x,2} \\ F_{x,3} \\ F_{x,4} \end{bmatrix} < \begin{bmatrix} F_{y,fmax}(t) \\ F_{y,rmax}(t) \\ F_{x1,max}(t) \\ F_{x2,max}(t) \\ F_{x3,max}(t) \\ F_{x4,max}(t) \end{bmatrix}. \quad (23)$$

The estimation of the maximal lateral tire forces is carried out by observation of the ICS of the front and rear tires. If the value of the ICS is lower than a certain percentage of the maximal ICS, then the lateral tire force value is used as maximal value for the allocation scheme. This method should avoid to allocate lateral tire force demand values from the allocation scheme that are not achievable due to tire force saturation.

The maximal longitudinal tire forces could be computed in a similar way by using the instantaneous driving stiffness. This will be topic of further research, for this contribution the maximal tire force are set to a predefined constant value. The allocation problem can be expressed as following:

$$\min_{\mathbf{u}} \mathbf{u}^T\mathbf{W}\mathbf{u} \quad \text{with} \quad \mathbf{v} = \mathbf{B}\mathbf{u}, \quad \mathbf{u}_{min}(t) \le \mathbf{u} \le \mathbf{u}_{max}(t) \quad (24)$$

The allocation problem is solved with Active Set algorithms and reduced to a Weighted Least Square (WLS) problem [14]:

$$\min_{\mathbf{u}} \mathbf{u}^T\mathbf{W}\mathbf{u} + \gamma_w\|\mathbf{B}\mathbf{u} - \mathbf{v}\|_T^2 \text{ subject to } \mathbf{u}_{min}(t) \le \mathbf{u} \le \mathbf{u}_{max}(t), \quad (25)$$

where the choice of γ_w must be well considered.

The matrix $\mathbf{W}$ can be used for additional criteria like tire work load minimization depending on what the allocated parameters are. Additionally each allocation equation can be weighted separately by an appropriate weighing matrix $\mathbf{T}$.